

# Anisotropic diffusion of metabolites in peripheral nerve using diffusion weighted magnetic resonance spectroscopy at ultra-high field

Jacob Ellegood<sup>a</sup>, Ryan T. McKay<sup>b</sup>, Chris C. Hanstock<sup>a</sup>, Christian Beaulieu<sup>a,\*</sup>

<sup>a</sup> Department of Biomedical Engineering, University of Alberta, 1098 Research Transition Facility, Edmonton, Alta., Canada T6G 2V2

<sup>b</sup> Canadian National High Field NMR Centre, University of Alberta, Edmonton, Alta., Canada

Received 6 June 2006; revised 25 August 2006

Available online 5 October 2006

## Abstract

Although the diffusivity and anisotropy of water has been investigated thoroughly in ordered axonal systems (i.e., nervous tissue), there have been very few studies on the directional dependence of diffusion of metabolites. In this study, the mean apparent diffusion coefficient (Trace/3 ADC) and fractional anisotropy (FA) values of the intracellular metabolites *N*-acetyl aspartate (NAA), creatine and phosphocreatine (tCr), choline (Cho), taurine (Tau), and glutamate and glutamine (Glx) were measured parallel and perpendicular to the length of excised frog sciatic nerve using a water suppressed, diffusion-weighted, spin-echo pulse sequence at 18.8 T. The degree of anisotropy (FA) of NAA ( $0.41 \pm 0.09$ ) was determined to be less than tCr ( $0.59 \pm 0.07$ ) and Cho ( $0.61 \pm 0.11$ ), which is consistent with previously reported human studies of white matter. In contrast, Glx diffusion was found to be almost isotropic with an FA value of  $0.20 \pm 0.06$ . The differences of FA between the metabolites is most likely due to their differing micro-environments and could be beneficial as an indicator of compartment specific changes with disease, information not readily available with water diffusion.

© 2006 Elsevier Inc. All rights reserved.

**Keywords:** Diffusion spectroscopy; Sciatic nerve; DTI; Diffusion tensor imaging

## 1. Introduction

Magnetic resonance is well established for measuring diffusion properties of water in the human brain and neural tissue. In 1990, the diffusion behavior of water was examined in the cat central nervous system by using diffusion-weighted magnetic resonance imaging with the diffusion sensitization gradients applied in different directions (*X*, *Y*, and *Z*) [1]. Faster diffusion (i.e. greater signal attenuation) was noted parallel (versus perpendicular) to the white matter tracts in cat brain and this was termed anisotropic diffusion. Diffusion anisotropy of water in neural tissue has been examined quite extensively since that date, but particularly after the introduction of diffusion tensor imaging (DTI) in 1994 [2,3], and more recently this fundamental

property of water in white matter has been used to perform 3D tractography of the fibers in the brain [4–7]. DTI of tissue water includes contributions from exchanging intra- and extracellular water, which makes compartment specific interpretation of diffusion characteristics rather complex. It has long been shown that reductions in water diffusion are a sensitive indicator of early cerebral ischemia [8], and despite the theory that this decrease is due to a water shift from extra-cellular to intra-cellular space, purely intracellular metabolites also show a reduction of diffusion by a similar magnitude without any compartmental shifts [9–15]. These metabolite diffusion studies are usually interested in either single direction diffusion or rotationally invariant mean diffusivity.

To date, there have only been two published human studies that have studied anisotropic diffusion of intracellular metabolites in tissue [16,17]. One study measured the ADC of NAA parallel and perpendicular to the corpus

\* Corresponding author. Fax: +1 780 492 8259.

E-mail address: [christian.beaulieu@ualberta.ca](mailto:christian.beaulieu@ualberta.ca) (C. Beaulieu).

callosum in the normal human brain at 1.5 T and found the ADC parallel to be  $\sim 2$ – $3$  times greater than the ADC perpendicular [16]; however they examined only two human volunteers and measured only one metabolite, NAA. More recently the full diffusion tensor of gray and white matter in the normal human brain at 3 T was examined [17] and indicated that the fractional anisotropy of tCr ( $0.66 \pm 0.13$ ) and Cho ( $0.67 \pm 0.14$ ) was significantly higher than NAA ( $0.56 \pm 0.13$ , tCr  $p = 0.001$  and Cho  $p = 0.001$ , paired  $t$ -test), which may seem counterintuitive since tCr and Cho are not solely located in the axons (presumably highly anisotropic) as is NAA but rather are also found in environments expected to be more isotropic such as astrocytes and oligodendrocytes [18].

Accurate in vivo DW-MRS measurements are quite challenging due to subject movement, shimming issues, low SNR, and large voxel sizes that include a variety of distinct neural structures. A model system, such as an excised sciatic nerve, eliminates all of those factors. In such a preparation, the nerve is aligned and fixed in position which yields a better shim, much more time available to average, and permits observation of a single well defined structure (a bundle of axons). Also, the size of the nerve allows the use of a spectrometer with a magnetic field strength much higher than used in vivo. The anisotropy of the intracellular metabolites *N*-acetyl aspartate (NAA), creatine and phosphocreatine (tCr), and choline (Cho) have been measured previously in the excised bovine optic nerve at 11.7 T [19]. The ADC values were measured parallel and perpendicular to the long axis of the optic nerve using extremely high  $b$ -values (100,000–300,000 s/mm<sup>2</sup>), and the diffusion decay curves were fit to a bi-exponential. The diffusion attenuation curves varied with diffusion gradient direction for NAA, tCr, and Cho; however the focus of that study was on  $q$ -space analysis at extremely high  $b$ -value, and therefore differences in diffusion with direction at lower  $b$ -values were not examined. The purpose of this paper was to examine the anisotropic diffusion of the three main metabolites (NAA, tCr, and Cho), as well as any other measurable metabolites, in the excised frog sciatic nerve, with the ultimate goal to relate this information to the anisotropic nature of the metabolite diffusion in the white matter of the human brain.

## 2. Methods

### 2.1. Nerve sample preparation

All sciatic nerve samples were taken from adult *Xenopus laevis*, the African clawed frog, which had been housed in an aquatic environment at room temperature. In total, nine nerve samples from five frogs were used in this study. Following euthanasia in MS-222 (3-aminobenzoic acid ethyl ester),  $\sim 3$  cm segments of nerve were removed and placed in an oxygenated physiological buffer (112 mM NaCl, 3.0 mM KCl, 1.6 mM MgSO<sub>4</sub>, 3.0 mM CaCl<sub>2</sub>, 5.0 mM glucose, 3.0 mM HEPES). The perineurial sheath surrounding

the nerve was removed from all nerve samples. The nerve samples were immersed in Fluorinert (FC-77, Sigma-Aldrich Canada Ltd. Oakville, Ontario, Canada) and were aligned along the Z-axis of the magnet by tying thread to one end and pulling the nerve (and Fluorinert) into a small capillary tube (1 mm inner diameter) after which both ends were sealed with parafilm. The capillary tube was then oriented within a Wilmad 535P-5 mm NMR tube along the Z-axis and was surrounded by 99% D<sub>2</sub>O (required for the lock signal, Fig. 1). All nerve samples were placed in the NMR between 45 min and 3 h of extraction.

### 2.2. NMR experiments

An 800 MHz (18.8 T) Varian Inova NMR spectrometer running VNMRJ 1.1D equipped with a XYZ-gradient HCN 5 mm probe with a maximum gradient strength of  $\sim 30$  G/cm along the  $X$  and  $Y$  axes and  $\sim 60$  G/cm along the  $Z$ -axis, was used for all diffusion experiments. A diffusion-weighted spin-echo pulse sequence with 5.0 ms diffusion gradient pulses ( $\delta$ ) and a diffusion gradient separation ( $\Delta$ ) of 20.0 ms yielded a diffusion time ( $\Delta - \delta/3$ ) of 18.3 ms. Sequence parameters were as follows: TE = 30 ms, TR = 3 s, SW = 12,000 Hz, number of complex points = 24,002. Water suppression was achieved using a water selective 90° shaped Gaussian pulse prior to the hard 90 in the spin-echo pulse sequence. The gradient strengths of the  $X$ ,  $Y$ , and  $Z$  gradients were calibrated based on a Cr diffusion coefficient of  $0.80 \times 10^{-3}$  mm<sup>2</sup>/s at 20 °C [20] using a 600  $\mu$ L phantom containing NAA (3 mM), Cr (3 mM), and Cho (1 mM). Seven separate calibrated  $b$ -values were measured for each direction (227, 539, 903, 1107, 1444, 1710,

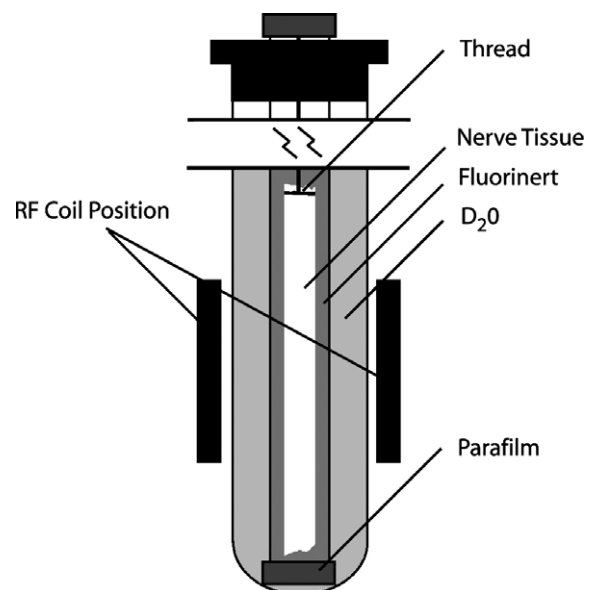


Fig. 1. Diagram of the setup for the 5 mm NMR tube. The excised sciatic nerve of the frog was immersed in a fluorinated compound to prevent dehydration and placed in a 1 mm inner diameter capillary tube, which was aligned parallel to the Z-axis of the magnet. The capillary tube was surrounded by 99% D<sub>2</sub>O, which was required for the lock signal.

and 1970 s/mm<sup>2</sup> for the *X*-direction, 235, 530, 796, 1063, 1382, 1626, and 1871 s/mm<sup>2</sup> for the *Y*-direction, and 245, 689, 1046, 1305, 1662, 1949, and 2322 s/mm<sup>2</sup> for the *Z*-direction). A temperature of 20 °C was used for both phantom and nerve experiments.

A 1 Hz exponential filter was used during spectral processing. The shimmed linewidth at half height for the NAA peak was  $5 \pm 3$  Hz. The apparent diffusion coefficients were calculated by measuring the slope of  $\ln(\text{signal intensity})$  versus *b*-value. The signal intensity was calculated using a home built Matlab program, and was a measure of the amplitude of the maximum value of the peak relative to a fitted baseline through the peak. The fitted baseline consisted of a straight line fit through points adjacent to both sides of the designated peak. The phantom study on NAA, Cr, and Cho was repeated three times to ensure the accuracy of the *b*-value calibration for each gradient direction. ADC values were measured in the *X*, *Y*, and *Z* directions from separate samples ( $N = 1$ ) of phosphocreatine (PCr), taurine (Tau), glutamate, and glutamine that were not included in the original calibration. Diffusion experiments in the phantoms acquired 16 averages. The diffusion coefficients of NAA, Cr, and Cho in the *X*, *Y*, and *Z* directions as well as the mean diffusivity, i.e., Trace/3 ADC, were consistent with previously reported phantom diffusion coefficients [20], and the low FA values of 0.01–0.08 for all metabolites showed the expected isotropy (Table 1).

Nerve experiments were performed using the same *b*-values used in the calibration study (listed previously). The number of averaged transients used in the nerve experiments ranged from 64 to 512, with more averages being used to examine peaks of lower SNR. The total scan time for the 64 average experiments was ~90 min. Since the excised nerve axis was aligned with the laboratory frame, the apparent diffusion coefficient (ADC) measured along the *Z*-axis corresponds to the largest eigenvalue (i.e., parallel diffusion), whereas the ADC values along the two orthogonal axes correspond to the two smaller eigenvalues (i.e., perpendicular diffusion) of the diffusion tensor. The mean diffusivity (Trace/3 ADC) and the fractional anisotropy (FA) were calculated from these eigenvalues. It has been shown previously that ~18 metabolites are visible in the rat brain at 9.4 T with a TE of 2 ms [21]; however,

due to problems such as J-modulation and T<sub>2</sub> relaxation over the relatively long spin-echo time of 30 ms, only five metabolites were quantified in the frog sciatic nerve, namely NAA (2.01 ppm), tCr (3.03 ppm), Cho (3.21 ppm), Tau (3.25 ppm), and Glx (3.75 ppm, i.e., cannot distinguish glutamine and glutamate in this case). The assignment of metabolite peaks was based on previous literature [21] as well as individual metabolite spectra measured in aqueous phantom (spectra not shown). Glx was only visible in three and Tau in four nerve samples, respectively, likely due to a better shim, thicker nerve, and higher SNR in those cases. The Tau peak was hard to distinguish in the *Z*-direction at *b*-values larger than 1700 s/mm<sup>2</sup>; therefore, Tau had only five *b*-values used for ADC calculation in the *Z*-direction. Glx was not sensitive to this effect due to a smaller drop in amplitude for the Glx peak along *Z* with increasing *b*-values compared to the Tau peak.

In this paper, Cr and PCr were averaged together, by measuring the combined methyl peak at 3.03 ppm where there was no defined separation, to yield a measurement of tCr assuming that the diffusion coefficients of these two metabolites are similar in nerve. Note in fact that in an aqueous phantom, the diffusion of Cr and PCr are not the same, and neither are glutamate and glutamine (Table 1). Three of the nerve samples had sufficient spectral resolution that allowed the separation of the Cr and PCr peaks located at 3.91 ppm and 3.93 ppm, respectively, which are the resonances originating from the methylene protons of Cr/PCr. Examination of this data revealed PCr had a consistently higher ADC in the *Y*-direction when compared to the *X*-direction and Cr had a consistently higher ADC in the *X*-direction when compared to the *Y*. There is no reason to expect consistent differences between the perpendicular *X* and *Y* directions (not observed for other metabolites). Examination of the low diffusion-weighted ( $b \sim 200$  s/mm<sup>2</sup>) spectra for *X*, *Y*, and *Z* ADC measurements showed a reduction in the amplitude of the PCr peak located at 3.93 ppm over time and an increase in the intensity of the Cr peak located at 3.91 ppm (visible in Fig. 2, *Z*-direction measured prior to *Y*-direction). Thus the ADC measurements for Cr and PCr individually are corrupted due to changing concentrations of these two metabolites (lack of oxidative phosphorylation [22]) during the measurement. The diffusion measurements of the total

Table 1

Diffusion measurements of *N*-acetyl aspartate (NAA, 3 mM), creatine (Cr, 3 mM) and choline (Cho, 1 mM) combined in a 600  $\mu$ L aqueous solution ( $N = 3$ ), and phosphocreatine, taurine, glutamate, and glutamine (all 25 mM) in separate 600  $\mu$ L aqueous solutions ( $N = 1$ )

Metabolite	Apparent diffusion coefficient ( $\times 10^{-3}$ mm <sup>2</sup> /s)				Fractional anisotropy
	<i>X</i>	<i>Y</i>	<i>Z</i>	Trace/3	
<i>N</i> -Acetyl aspartate ( $N = 3$ )	0.64 $\pm$ 0.08	0.66 $\pm$ 0.10	0.65 $\pm$ 0.02	0.65 $\pm$ 0.05	0.08 $\pm$ 0.02
Creatine ( $N = 3$ )	0.80 $\pm$ 0.02	0.84 $\pm$ 0.05	0.80 $\pm$ 0.05	0.82 $\pm$ 0.01	0.06 $\pm$ 0.01
Phosphocreatine ( $N = 1$ )	0.51	0.51	0.57	0.53	0.07
Choline ( $N = 3$ )	0.94 $\pm$ 0.02	0.98 $\pm$ 0.02	0.98 $\pm$ 0.02	0.97 $\pm$ 0.01	0.03 $\pm$ 0.01
Taurine ( $N = 1$ )	1.00	1.05	0.98	1.01	0.03
Glutamate ( $N = 1$ )	0.68	0.70	0.68	0.68	0.01
Glutamine ( $N = 1$ )	0.79	0.85	0.74	0.79	0.07

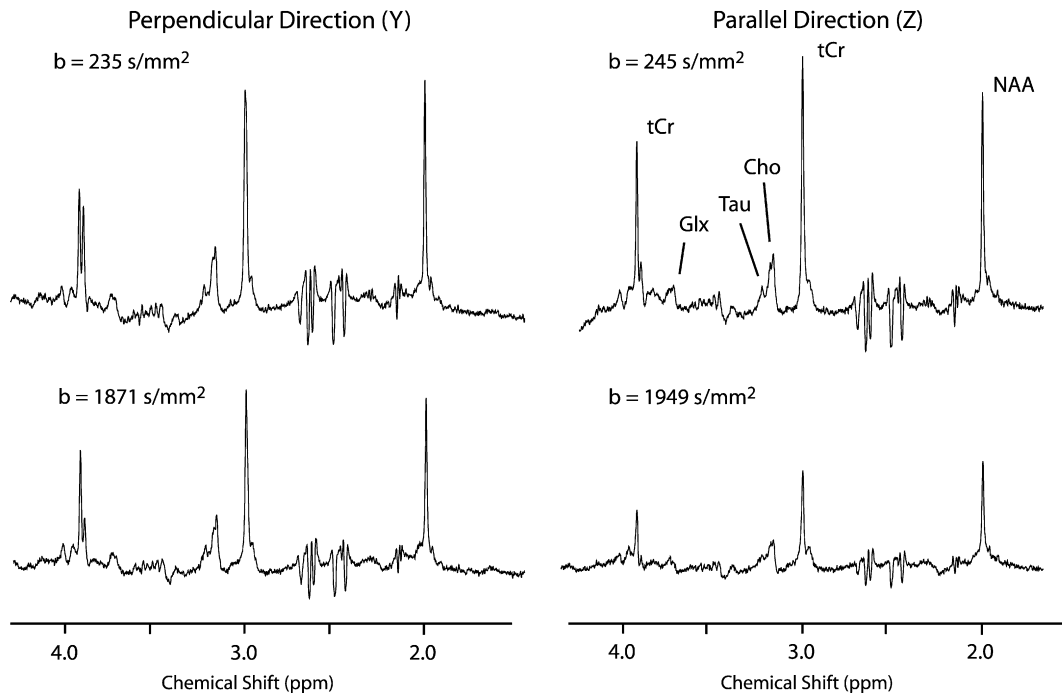


Fig. 2. Example spectra (TE = 30 ms) from low (235 and 245 s/mm<sup>2</sup>) and high  $b$ -values (1871 and 1949 s/mm<sup>2</sup>) in the perpendicular ( $Y$ ) and parallel ( $Z$ ) directions in excised frog sciatic nerve. It can clearly be seen that the signal intensity in the parallel diffusion ( $Z$ ) direction decays faster than the signal intensity in the perpendicular diffusion ( $Y$ ) direction. Contrary to what is seen in human brain spectra, where NAA is the largest peak, in the peripheral nerve tCr is the largest peak in the spectrum. Also, note that differences in tCr appearance at  $\sim 3.9$  ppm at low  $b$ -value between  $Z$  (measured earlier) and  $Y$  (measured later) is caused by changes in the concentration of PCr (left peak decreasing) and Cr (right peak increasing) after excision of the nerve (see Section 2).

creatine peak, including both PCr and Cr, were deemed reasonable given the consistency of the total creatine area over the entire experiment. Each individual nerve was scanned at  $b = 0$  s/mm<sup>2</sup> at both the beginning and the end of the scan session. Changes in the metabolite peak area at these two time points, are expressed as mean  $\pm$  SD percent values as follows: NAA =  $0.6 \pm 4.0\%$ , tCr =  $0.0 \pm 3.4\%$ , Cho =  $1.8 \pm 7.0\%$ , Tau =  $-1.6 \pm 5.7\%$ , and Glx =  $2.6 \pm 2.8\%$ ; therefore, there are no significant differences of peak area before and after for any metabolite (paired  $t$ -test).

### 3. Results

Table 1 lists the ADC values in the  $X$ ,  $Y$ , and  $Z$  directions of NAA, Cr, PCr, Cho, Tau, Glu, and Gln each measured in a 600  $\mu$ L isotropic phantom. NAA, Cr and Cho were combined in a single phantom used for calibration of the gradients and their Trace/3 ADC values in the phantom were determined to be  $0.65 \pm 0.05 \times 10^{-3}$  mm<sup>2</sup>/s,  $0.82 \pm 0.01 \times 10^{-3}$  mm<sup>2</sup>/s, and  $0.97 \pm 0.01 \times 10^{-3}$  mm<sup>2</sup>/s for NAA, Cr, and Cho, respectively, which is consistent with previous literature values [20]. The low FA values of 0.01–0.08 indicate isotropic diffusion, although the observed small differences between  $X$ ,  $Y$ , and  $Z$  ADC values in the phantom are due to noise.

Example <sup>1</sup>H nerve spectra are shown in Fig. 2, with diffusion gradients either perpendicular ( $Y$ -direction) or par-

allel ( $Z$ -direction) to the long axis of the nerve at low (235 and 245 s/mm<sup>2</sup>) and high (1871 and 1949 s/mm<sup>2</sup> for  $Y$  and  $Z$ , respectively)  $b$ -values at 18.8 T. Note that contrary to human brain spectra, tCr has a higher concentration when compared to NAA in the frog sciatic nerve. Spectral acquisitions yielded average signal to noise ratios for the 64 average spectra of  $48 \pm 23$ ,  $57 \pm 29$ ,  $22 \pm 10$ ,  $11 \pm 2$ , and 11 for the NAA, tCr, Cho, Tau, and Glx peaks, respectively at the lowest  $b$ -value spectra in the  $X$ -direction in the nerves. Glx was only observed in one of the 64 average spectra, hence the lack of a standard deviation (it was found in two other spectra with more averages). The peaks of NAA, Cr, and Cho can clearly be seen, as well as the corresponding linear decay with increasing  $b$  value. Fig. 3 displays the diffusion decay curves for the phantom (A) and the five metabolites, NAA (B), tCr (C), Cho (D), Tau (E), and Glx (F) in the nerve along the  $X$ ,  $Y$  and  $Z$  directions. Note the greater signal attenuation at higher  $b$ -value in the  $Z$ -direction in Figs. 3B–E indicating faster diffusion along the length of the nerve samples. Faster  $Z$ -diffusion is not evident in the Glx decay curves (Fig. 3F).

The Trace/3 ADC and FA values of NAA, tCr, Cho, Tau, and Glx measured in the frog sciatic nerve are listed in Table 2. The Trace/3 ADC values ranged from 0.19 to  $0.26 \times 10^{-3}$  mm<sup>2</sup>/s ( $0.22 \pm 0.02 \times 10^{-3}$  mm<sup>2</sup>/s, mean  $\pm$  SD) for NAA,  $0.23$ – $0.33 \times 10^{-3}$  mm<sup>2</sup>/s ( $0.28 \pm 0.03 \times 10^{-3}$  mm<sup>2</sup>/s) for tCr,  $0.13$ – $0.20 \times 10^{-3}$  mm<sup>2</sup>/s ( $0.16 \pm 0.02 \times 10^{-3}$  mm<sup>2</sup>/s) for Cho,  $0.21$ – $0.29 \times 10^{-3}$  mm<sup>2</sup>/s ( $0.25 \pm$

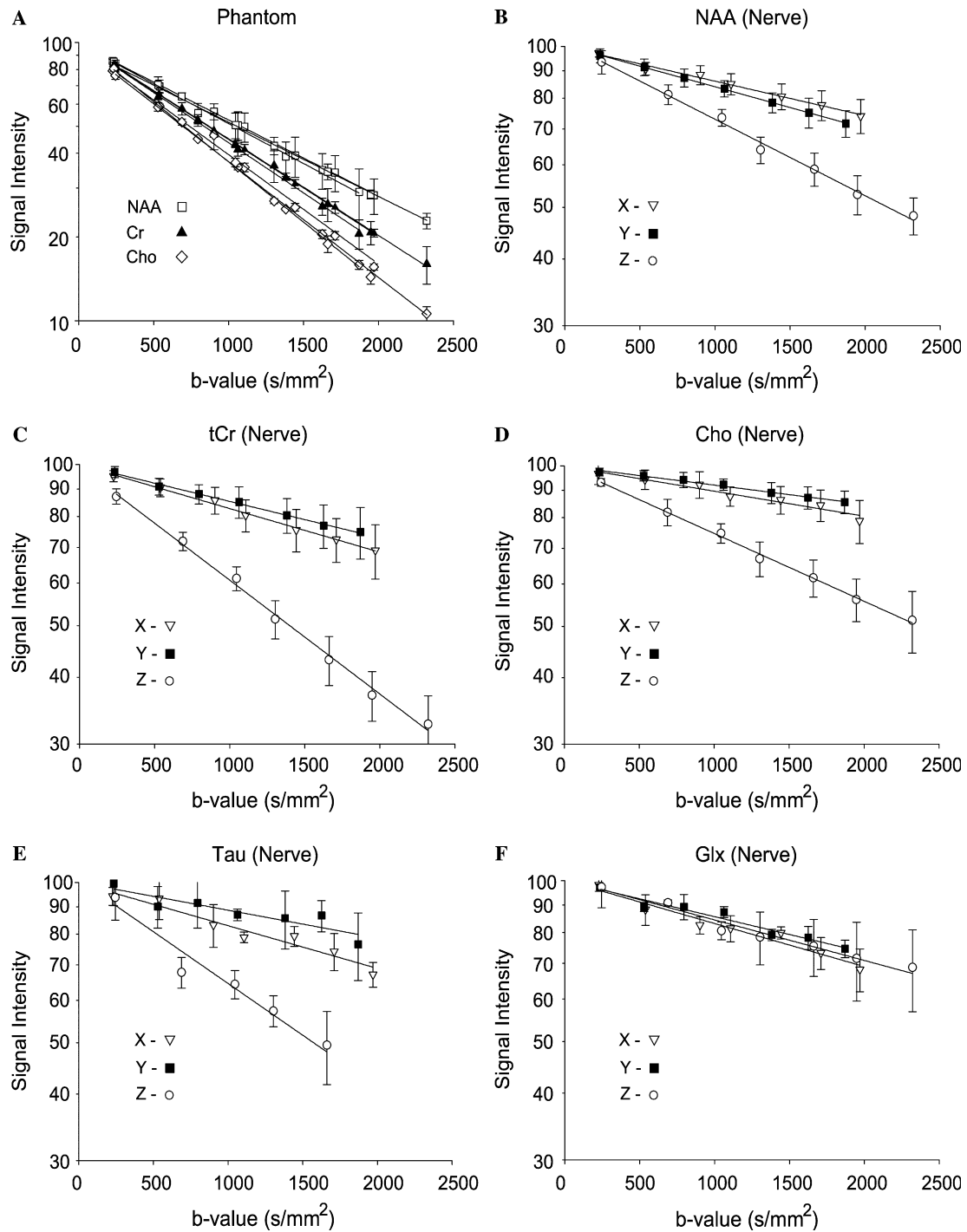


Fig. 3. Decay curve for (A) an aqueous solution ( $N = 3$ ) of NAA, Cr, and Cho which demonstrated isotropic diffusion ( $X$ ,  $Y$ , and  $Z$  curves all shown) and (B) NAA ( $N = 9$ ), (C) tCr ( $N = 9$ ), (D) Cho ( $N = 9$ ), (E) Tau ( $N = 4$ ), and (F) Glx ( $N = 3$ ) in peripheral nerve in the perpendicular ( $X$ ,  $Y$ ) and parallel ( $Z$ ) directions. In the parallel  $Z$ -direction, the faster diffusion can clearly be seen in the nerve for all metabolites except Glx. The tCr parallel diffusion is the fastest, and the Cho perpendicular diffusion is the slowest. Tau also demonstrates considerable anisotropy whereas Glx appears isotropic. The error bars reflect the standard deviation of the signal intensity over all nerve samples at each  $b$ -value.

$0.03 \times 10^{-3} \text{ mm}^2/\text{s}$  for Tau, and  $0.13\text{--}0.19 \times 10^{-3} \text{ mm}^2/\text{s}$  ( $0.17 \pm 0.03 \times 10^{-3} \text{ mm}^2/\text{s}$ ) for Glx. The FA values ranged from 0.26 to 0.57 ( $0.41 \pm 0.09$ , mean  $\pm$  SD) for NAA, 0.44–0.67 ( $0.59 \pm 0.07$ ) for tCr, 0.44–0.76 ( $0.61 \pm 0.11$ ) for Cho, 0.52–0.73 ( $0.60 \pm 0.10$ ) for Tau, and 0.15–0.26 ( $0.20 \pm 0.06$ ) for Glx.

The  $r^2$  values for the signal attenuation curves of the nine nerve samples ranged from 0.90 to 1.00 ( $0.98 \pm 0.03$ , mean  $\pm$  SD) for NAA, 0.73–1.00 ( $0.96 \pm 0.06$ ) for tCr, and 0.50–1.00 ( $0.84 \pm 0.16$ ) for Cho. The lower average  $r^2$  value for Cho probably is due to the lower SNR of Cho compared to the other two metabolites. With the even



Table 2

ADC values perpendicular (*X* and *Y*) and parallel (*Z*) to the long axis of the frog sciatic nerve as well as derived diffusion parameters, Trace/3 ADC and fractional anisotropy

Metabolite	Apparent diffusion coefficient ( $\times 10^{-3}$ mm <sup>2</sup> /s)				Fractional anisotropy
	<i>X</i>	<i>Y</i>	<i>Z</i>	Trace/3	
NAA ( <i>N</i> = 9)	0.15 ± 0.04	0.18 ± 0.03	0.33 ± 0.04	0.22 ± 0.02	0.41 ± 0.09
Total creatine ( <i>N</i> = 9)	0.19 ± 0.06	0.16 ± 0.06	0.49 ± 0.05	0.28 ± 0.03	0.59 ± 0.07
Choline ( <i>N</i> = 9)	0.11 ± 0.04	0.08 ± 0.02	0.29 ± 0.05	0.16 ± 0.02	0.61 ± 0.11
Taurine ( <i>N</i> = 4)	0.19 ± 0.02	0.12 ± 0.06	0.44 ± 0.03	0.25 ± 0.03	0.60 ± 0.10
Glutamate/glutamine ( <i>N</i> = 3)	0.19 ± 0.04	0.15 ± 0.02	0.17 ± 0.07	0.17 ± 0.03	0.20 ± 0.06

lower SNR data of the coupled peaks (Tau and Glx), the  $r^2$  values ranged from 0.45 to 0.93 ( $0.76 \pm 0.16$ ) for Tau and 0.65–0.97 ( $0.88 \pm 0.09$ ) for Glx.

#### 4. Discussion

Previous water diffusion measurements in the excised frog sciatic nerve have reported a Trace/3 ADC value of  $0.76 \times 10^{-3}$  mm<sup>2</sup>/s for water [23], which is  $\sim 3.5$  times larger than the Trace/3 ADC value of ( $0.22 \pm 0.02 \times 10^{-3}$  mm<sup>2</sup>/s) for NAA reported in the current study. The Trace/3 ADC of NAA in excised frog sciatic nerve is consistent with the NAA Trace/3 ADC value found in the corpus callosum of the two previous human studies  $0.20 \pm 0.02 \times 10^{-3}$  mm<sup>2</sup>/s [17] and 0.18 or  $0.20 \times 10^{-3}$  mm<sup>2</sup>/s (pseudo Trace/3 ADC) [16]. However, one should be aware that these ADC measurements were taken at different temperatures, with the in vitro frog nerve being measured at room temperature (20 °C) while the in vivo human brain was measured at physiological temperature (37 °C). The lower temperature of 20 °C used in this study would cause the ADC of the metabolites examined to be lower than they would be at physiological temperature of the human brain. Also, the ADC values of the metabolites in in vitro frog nerve could theoretically be less than in vivo prior to excision given the known reductions ( $\sim 30\%$ ) in metabolite ADC after stroke in rodent models [9–15]. Furthermore, studies in rat trigeminal nerve have shown an  $\sim 20\%$  decrease in pseudo Trace/3 ADC of water post mortem [24], so a similar decrease might be expected for metabolites in excised nerve. However, an in vivo measurement in vivo frog sciatic nerve with the vertical bore 800 MHz spectrometer is not possible. Given both factors of lower temperature and ischemic effects, yet similar Trace/3 ADC values in in vitro frog sciatic nerve and human brain white matter, the metabolites in frog sciatic nerve are likely more mobile than in human corpus callosum (assuming same temperature). This is presumably due to the frog sciatic nerve consisting of larger axons (typically 4–10  $\mu$ m, some 15–20  $\mu$ m) [23,25] that are also less densely packed than the smaller axons of the corpus callosum (1–3  $\mu$ m) [26].

With regard to the singlet metabolites, the Cho Trace/3 ADC in this study tends to be the smallest ( $p < 0.001$  versus tCr and  $p < 0.001$  versus NAA) followed by NAA ( $p < 0.01$  versus tCr) and then the tCr ADC is the highest. This is contrary to what was seen in our previous human brain

paper, where the Trace/3 ADC trend was  $NAA < tCr \sim Cho$  [27]. However, a recent survey of different studies of metabolite diffusion has suggested that the actual value of the mean diffusivity of Cho may be affected by the echo time of the acquisition, with shorter echo times yielding lower ADC values [28]. The mean diffusivity of Cho in the nerve is reduced to the largest extent relative to its diffusion in a phantom of bulk water (84% reduction for Cho versus 66% for NAA). The Tau Trace/3 ADC ( $0.25 \pm 0.03 \times 10^{-3}$  mm<sup>2</sup>/s) is consistent with the other Trace/3 ADC values in nerve. Two previous studies have reported single direction ADC values for Tau and Glu in rat brain in vivo [15,29]. The ADC values for Tau were  $0.103 \pm 0.003 \times 10^{-3}$  mm<sup>2</sup>/s [29] and  $0.198 \pm 0.059 \times 10^{-3}$  mm<sup>2</sup>/s [15] at 37 °C. These values are smaller than those reported from the frog sciatic nerve at 20 °C; however they were only measured in one direction and in a region containing a variety of different structures. The ADC values for Glu from those studies were  $0.112 \pm 0.002 \times 10^{-3}$  mm<sup>2</sup>/s [29] and  $0.147 \pm 0.021 \times 10^{-3}$  mm<sup>2</sup>/s [15], the first being smaller and the second falling within the range of our value in nerve  $0.17 \pm 0.03 \times 10^{-3}$  mm<sup>2</sup>/s. A recent study on primate brain has reported single direction ADC values for Glu of  $0.21 \times 10^{-3}$  mm<sup>2</sup>/s [30], which is larger than what has been shown previously in the rat brain, but is consistent with what has been shown in this study for Glx. Similar to the NAA discussion above, absolute ADC comparisons between studies are complicated by measurements at different temperatures as well as the in vivo versus in vitro issue.

The parallel diffusion, in our current study, is significantly greater for four of the five metabolites measured when compared with perpendicular diffusion, with  $p$ -values ranging from  $1.6 \times 10^{-5}$  to  $7.0 \times 10^{-7}$ , Glx being the exception showing no significant directional preference. The average parallel diffusion of NAA was  $0.33 \pm 0.04 \times 10^{-3}$  mm<sup>2</sup>/s and the average perpendicular diffusion (average of *X* and *Y* combined) of NAA was  $0.17 \pm 0.03 \times 10^{-3}$  mm<sup>2</sup>/s, which yielded a parallel over perpendicular ratio of  $2.0 \pm 0.3$ . The other parallel over perpendicular diffusion ratios were determined to be  $2.9 \pm 0.4$  for tCr,  $3.2 \pm 1.0$ , for Cho, and  $3.0 \pm 0.7$  for Tau. The interesting finding was the low anisotropy of Glx indicated by a parallel over perpendicular ratio of  $1.0 \pm 0.4$ . Two human studies have also reported similar parallel over perpendicular diffusion ratios of NAA in the white matter of the human

brain. One study measured the ADC value of NAA in the corpus callosum of the human brain of two healthy volunteers, and found that the ADC value measured parallel to the fibers in the corpus callosum ( $0.33$  and  $0.30 \times 10^{-3} \text{ mm}^2/\text{s}$ ) was  $\sim 2$ – $3$  times greater than the ADC value measured perpendicular ( $0.10$  and  $0.15 \times 10^{-3} \text{ mm}^2/\text{s}$ ) [16]; the other study measured eigenvalues for four different large white matter structures in the human brain and found parallel over perpendicular ADC ratios of 2.1–2.8 for NAA, 2.5–3.7 for tCr, and 2.5–3.7 for Cho [17], which are consistent with the singlet metabolite ADC ratios measured in the peripheral nerve.

The FA values in the frog sciatic nerve were ordered  $\text{Glx} \ll \text{NAA} < \text{tCr} \sim \text{Cho} \sim \text{Tau}$  and ranged from 0.20 to 0.62, which are lower than FA values of water previously reported in the frog sciatic nerve of 0.73 (extrapolated assuming  $\lambda_1 = \text{parallel ADC}$  and  $\lambda_2 = \lambda_3 = \text{perpendicular ADC}$ ) [23]. A previous study that calculated FA values in four different white matter regions in the human brain found that the FA of NAA was significantly less than tCr and Cho in the white matter [17]. The primary cells in the peripheral nerve are Schwann cells and the axons of the dorsal root ganglion neurons. In cell cultures of these cell lines it was shown that NAA was only found within the neurons, whereas Cr and Cho were found in both the neurons and Schwann cells [18]. In spite of the previous human study, it was expected that NAA, localized in the axonal compartment of the peripheral nerve, would have a larger FA than tCr and Cho because of the localization of tCr and Cho in Schwann cells, likely isotropic, in addition to axons. However, the FA value of NAA ( $0.41 \pm 0.09$ ) in peripheral nerve was found to be significantly less than tCr ( $0.59 \pm 0.07$ ) and Cho ( $0.61 \pm 0.11$ ) ( $p = 0.0002$  and  $p = 0.02$ , respectively).

In the previous human study it was thought that the higher FA of tCr and Cho might be a result of the lower SNR in the human brain of tCr and Cho when compared to NAA; however that is not the case in the peripheral nerve where tCr has the highest SNR among the metabolites. The higher tCr FA arises from tCr having a much larger parallel ADC ( $Z$ ) than NAA ( $0.49 \pm 0.05 \times 10^{-3} \text{ mm}^2/\text{s}$  versus  $0.33 \pm 0.04 \times 10^{-3} \text{ mm}^2/\text{s}$ ), which could be an extension of the faster diffusion of tCr in unrestricted bulk water and the difference in molecular weight (175.1 g/mol for NAA, and 149.2 g/mol for Cr). The perpendicular diffusion ( $X$  and  $Y$ ) of NAA and tCr are very similar ( $0.17 \pm 0.03 \times 10^{-3} \text{ mm}^2/\text{s}$  for NAA and  $0.18 \pm 0.06 \times 10^{-3} \text{ mm}^2/\text{s}$  for tCr) and show no significant differences, which may indicate a similar restriction in the perpendicular direction. Cho also has a larger FA than NAA in the frog sciatic nerve. This difference arises from the much smaller perpendicular ADC values ( $X$  and  $Y$ ) of Cho ( $0.10 \pm 0.04 \times 10^{-3} \text{ mm}^2/\text{s}$ ) versus that of NAA ( $0.17 \pm 0.03 \times 10^{-3} \text{ mm}^2/\text{s}$ ), which is opposite from what is seen with tCr, while Cho and NAA have similar parallel diffusivities (Table 2). Choline diffuses faster in bulk water than both NAA and Cr; however, the similar parallel diffusion

of Cho to NAA, and the much lower perpendicular diffusion, would seem to indicate that Cho diffusion is further hindered in the nerve, perhaps because of the close association of Cho with membranes. Previous work which measured the diffusion of metabolites parallel and perpendicular to white matter tracts in the human corpus callosum and cortical spinal tract show also that tCr in the white matter has a larger parallel diffusion when compared to NAA but the human study did not show a smaller perpendicular diffusion for Cho when compared to NAA [17]. The Tau FA value ( $0.60 \pm 0.10$ ) was consistent with the FA values of tCr and Cho, with Tau having a similar parallel ( $0.44 \pm 0.03 \times 10^{-3} \text{ mm}^2/\text{s}$ ) and perpendicular ( $0.15 \pm 0.05 \times 10^{-3} \text{ mm}^2/\text{s}$ ) ADC value as tCr. Glx on the other hand had a much smaller FA value,  $0.20 \pm 0.06$ , which indicated that it is in an isotropic environment when compared with the other metabolites.

The measurement of the Trace/3 ADC and FA of the lower SNR metabolites Tau and Glx are certainly open to discussion as the measurement of these metabolites proved to be challenging. Although Tau tended to follow trends in FA and Trace/3 ADC that were similar to what is seen with the main singlet metabolites (NAA, tCr, and Cho), Glx did not. The low FA value of Glx in the peripheral nerve,  $0.20 \pm 0.06$ , was unexpected but interesting, and thus questions arise about the accuracy of the measurement. The ADC was calculated by measuring the slope of  $\ln(\text{signal intensity})$  versus  $b$ -value, and while this is entirely valid and reproducible for the strong singlet resonances, perhaps it may be more accurate to measure the slope of the  $\ln(\text{signal area of peak})$  versus  $b$ -value for a broad multiplet. The area under the Glx peak was measured for each  $b$ -value of the three nerve samples where Glx was detected. The diffusion parameters resulting from the two methods (area versus peak height) were not statistically different; however more testing, with a greater number of samples, in a different environment (brain), and possibly even with a sequence optimized for the detection of glutamate and/or glutamine needs to be examined to confirm this result. This may be difficult given the challenges associated with measuring ADC from the coupled resonance peaks. If the observation of a reduced FA holds up to future scrutiny, a possible explanation for Glx having a low FA could be that the majority of Glx is located within the Schwann cells as well as perhaps some in the synaptic vesicles (isotropic environment) within the axons. Since the Schwann cells have been shown in immunohistochemical studies of the peripheral nerve to contain the majority of glutamine and glutamine related synthetase [31], it is possible that most of the Glx peak we are measuring derives from glutamine located mainly in the Schwann cells.

When interpreting the data in this study one must keep in mind some of the limitations. This frog nerve study was an in vitro preparation and thus was performed at a lower temperature than previous diffusion studies of neurological tissue in vivo. It should also be noted that even if there is no change in the concentration of the metabolites before

and after the measurements (as reported in Section 2), there may be a gradual deterioration of the barriers between compartments over time after excision of the nerve. However, the linearity of the decay curves over time, and similar ADC values (no significant differences, paired *t*-test) measured at different times (30 min to 3 h apart) for both *X* and *Y* directions suggest that such effects were not apparent in our measurements. Previous animal and human studies have shown reductions in metabolite ADCs in ischemic brain [9–15,32]. Since we are working with excised tissue (i.e., ischemic) in this work, ADC values in our study may be lower than the actual ADC values in vivo. Differences between the frog sciatic nerve (model system) and intact human brain white matter do exist, such as axonal size, axonal density, and cells responsible for myelination (Schwann cells in the peripheral nervous system versus oligodendrocytes in the central nervous system). However, our results indicate that the anisotropic diffusion of metabolites is acting in a similar fashion for both frog and human nervous tissue.

## 5. Conclusions

The Trace/3 ADC and FA of NAA, tCr, Cho, Tau, and Glx were measured at 18.8 T in a model system of human brain white matter, the excised frog sciatic nerve. Mean diffusivity was lowest for Cho and Glx, whereas it was quite similar for NAA, tCr, and Tau. The degree of anisotropy of tCr and Cho was higher than for NAA in frog sciatic nerve, in agreement with previous human brain white matter findings. Although preliminary, the FA of Glx was much smaller than the other four metabolites, indicating near isotropic diffusion. The differences in FA amongst the metabolites likely reflect their unique microenvironments and could be beneficial as an indicator of compartment specific changes with disease.

## Acknowledgments

The authors would like to acknowledge support from Natural Sciences and Engineering Research Council of Canada (NSERC) for operating, the Alberta Heritage Foundation for Medical Research (AHFMR) and NSERC for salary, and Canadian Foundation for Innovation (CFI), Alberta Science and Research Authority (ASRA), University Hospital Foundation, and AHFMR for infrastructure support. The authors would like to thank Isidro Bonilla for performing the nerve extractions, Dr. Richard Snyder for providing the frogs, and Dr. Brian Sykes and the Canadian National High Field NMR Centre (NANUC) for their assistance and use of the facilities. Operation of NANUC is funded by CIHR, NSERC, and the University of Alberta.

## References

- [1] M.E. Moseley, Y. Cohen, J. Kucharczyk, J. Mintorovitch, H.S. Asgari, M.F. Wendland, J. Tsuruda, D. Norman, Diffusion-weighted MR imaging of anisotropic water diffusion in cat central nervous system, *Radiology* 176 (1990) 439–445.
- [2] P.J. Basser, J. Mattiello, D. LeBihan, MR diffusion tensor spectroscopy and imaging, *Biophys. J.* 66 (1994) 259–267.
- [3] P.J. Basser, J. Mattiello, D. LeBihan, Estimation of the effective self-diffusion tensor from the NMR spin echo, *J. Magn. Reson. B* 103 (1994) 247–254.
- [4] T.E. Conturo, N.F. Lori, T.S. Cull, E. Akbudak, A.Z. Snyder, J.S. Shimony, R.C. McKinstry, H. Burton, M.E. Raichle, Tracking neuronal fiber pathways in the living human brain, *Proc. Natl. Acad. Sci. USA* 96 (1999) 10422–10427.
- [5] R. Xue, P.C. van Zijl, B.J. Crain, M. Solaiyappan, S. Mori, In vivo three-dimensional reconstruction of rat brain axonal projections by diffusion tensor imaging, *Magn. Reson. Med.* 42 (1999) 1123–1127.
- [6] D.K. Jones, A. Simmons, S.C. Williams, M.A. Horsfield, Non-invasive assessment of axonal fiber connectivity in the human brain via diffusion tensor MRI, *Magn. Reson. Med.* 42 (1999) 37–41.
- [7] P.J. Basser, S. Pajevic, C. Pierpaoli, J. Duda, A. Aldroubi, In vivo fiber tractography using DT-MRI data, *Magn. Reson. Med.* 44 (2000) 625–632.
- [8] M.E. Moseley, Y. Cohen, J. Mintorovitch, L. Chileuitt, H. Shimizu, J. Kucharczyk, M.F. Wendland, P.R. Weinstein, Early detection of regional cerebral ischemia in cats: comparison of diffusion- and T2-weighted MRI and spectroscopy, *Magn. Reson. Med.* 14 (1990) 330–346.
- [9] K.D. Merboldt, D. Horstmann, W. Hanicke, H. Bruhn, J. Frahm, Molecular self-diffusion of intracellular metabolites in rat brain in vivo investigated by localized proton NMR diffusion spectroscopy, *Magn. Reson. Med.* 29 (1993) 125–129.
- [10] A. van der Toorn, H.B. Verheul, J.W. Berkelbach van der Sprenkel, C.A. Tulleken, K. Nicolay, Changes in metabolites and tissue water status after focal ischemia in cat brain assessed with localized proton MR spectroscopy, *Magn. Reson. Med.* 32 (1994) 685–691.
- [11] M. Wick, Y. Nagatomo, F. Prielmeier, J. Frahm, Alteration of intracellular metabolite diffusion in rat brain in vivo during ischemia and reperfusion, *Stroke* 26 (1995) 1930–1933 (discussion 1934).
- [12] A. van der Toorn, R.M. Dijkhuizen, C.A. Tulleken, K. Nicolay, Diffusion of metabolites in normal and ischemic rat brain measured by localized 1H MRS, *Magn. Reson. Med.* 36 (1996) 914–922.
- [13] R.M. Dijkhuizen, R.A. de Graaf, K.A. Tulleken, K. Nicolay, Changes in the diffusion of water and intracellular metabolites after excitotoxic injury and global ischemia in neonatal rat brain, *J. Cereb. Blood Flow Metab.* 19 (1999) 341–349.
- [14] O. Abe, T. Okubo, N. Hayashi, N. Saito, N. Iriguchi, I. Shirouzu, Y. Kojima, T. Masumoto, K. Ohtomo, Y. Sasaki, Temporal changes of the apparent diffusion coefficients of water and metabolites in rats with hemispheric infarction: experimental study of transhemispheric diaschisis in the contralateral hemisphere at 7 tesla, *J. Cereb. Blood Flow Metab.* 20 (2000) 726–735.
- [15] W. Dreher, E. Busch, D. Leibfritz, Changes in apparent diffusion coefficients of metabolites in rat brain after middle cerebral artery occlusion measured by proton magnetic resonance spectroscopy, *Magn. Reson. Med.* 45 (2001) 383–389.
- [16] C.D. Kroenke, J.J. Ackerman, D.A. Yablonskiy, On the nature of the NAA diffusion attenuated MR signal in the central nervous system, *Magn. Reson. Med.* 52 (2004) 1052–1059.
- [17] J. Ellegood, C.C. Hanstock, C. Beaulieu, Diffusion tensor spectroscopy (DTS) of human brain, *Magn. Reson. Med.* 55 (2006) 1–8.
- [18] K.K. Bhakoo, I.T. Williams, S.R. Williams, D.G. Gadian, M.D. Noble, Proton nuclear magnetic resonance spectroscopy of primary cells derived from nervous tissue, *J. Neurochem.* 66 (1996) 1254–1263.
- [19] Y. Assaf, Y. Cohen, Structural information in neuronal tissue as revealed by q-space diffusion NMR spectroscopy of metabolites in bovine optic nerve, *NMR Biomed.* 12 (1999) 335–344.
- [20] K. Nicolay, K.P. Braun, R.A. Graaf, R.M. Dijkhuizen, M.J. Kruijskamp, Diffusion NMR spectroscopy, *NMR Biomed.* 14 (2001) 94–111.



- [21] J. Pfeuffer, I. Tkac, S.W. Provencher, R. Gruetter, Toward an in vivo neurochemical profile: quantification of 18 metabolites in short-echo-time (1)H NMR spectra of the rat brain, *J. Magn. Reson.* 141 (1999) 104–120.
- [22] O.A. Petroff, T. Ogino, J.R. Alger, High-resolution proton magnetic resonance spectroscopy of rabbit brain: regional metabolite levels and postmortem changes, *J. Neurochem.* 51 (1988) 163–171.
- [23] C. Beaulieu, P.S. Allen, An in vitro evaluation of the effects of local magnetic-susceptibility-induced gradients on anisotropic water diffusion in nerve, *Magn. Reson. Med.* 36 (1996) 39–44.
- [24] M.D. Does, J.C. Gore, Compartmental study of diffusion and relaxation measured in vivo in normal and ischemic rat brain and trigeminal nerve, *Magn. Reson. Med.* 43 (2000) 837–844.
- [25] C. Beaulieu, M.D. Does, R.E. Snyder, P.S. Allen, Changes in water diffusion due to Wallerian degeneration in peripheral nerve, *Magn. Reson. Med.* 36 (1996) 627–631.
- [26] F. Aboitiz, A.B. Scheibel, R.S. Fisher, E. Zaidel, Fiber composition of the human corpus callosum, *Brain Res.* 598 (1992) 143–153.
- [27] J. Ellegood, C.C. Hanstock, C. Beaulieu, Trace apparent diffusion coefficients of metabolites in human brain using diffusion weighted magnetic resonance spectroscopy, *Magn. Reson. Med.* 53 (2005) 1025–1032.
- [28] J. Valette, M. Guillermier, L. Besret, P. Hantraye, G. Bloch, V. Lebon, Isoflurane strongly affects the diffusion of intracellular metabolites, as shown by (1)H nuclear magnetic resonance spectroscopy of the monkey brain, *J. Cereb. Blood Flow Metab.* (2006).
- [29] J. Pfeuffer, I. Tkac, R. Gruetter, Extracellular-intracellular distribution of glucose and lactate in the rat brain assessed noninvasively by diffusion-weighted 1H nuclear magnetic resonance spectroscopy in vivo, *J. Cereb. Blood Flow Metab.* 20 (2000) 736–746.
- [30] J. Valette, M. Guillermier, L. Besret, F. Boumezbeur, P. Hantraye, V. Lebon, Optimized diffusion-weighted spectroscopy for measuring brain glutamate apparent diffusion coefficient on a whole-body MR system, *NMR Biomed.* 18 (2005) 527–533.
- [31] K.E. Miller, B.A. Richards, R.M. Kriebel, Glutamine-, glutamine synthetase-, glutamate dehydrogenase- and pyruvate carboxylase-immunoreactivities in the rat dorsal root ganglion and peripheral nerve, *Brain Res.* 945 (2002) 202–211.
- [32] M. Harada, M. Uno, F. Hong, S. Hisaoka, H. Nishitani, T. Matsuda, Diffusion-weighted in vivo localized proton MR spectroscopy of human cerebral ischemia and tumor, *NMR Biomed.* 15 (2002) 69–74.